Title
Next-generation sequencing identifies rare variants associated with Noonan syndrome

Permalink

Journal

ISSN

Authors
Chen, Peng-Chieh
Yin, Jiani
Yu, Hui-Wen
et al.

Publication Date

DOI

Peer reviewed

Next-generation sequencing identifies rare variants associated with Noonan syndrome

Peng-Chieh Chen[a,b,c], Jiani Yin[d], Hui-Wen Yu[c], Tao Yuan[b], Minerva Fernandez[d], Christina K. Yung[e], Quang M. Trinh[e], Vanya D. Peltekova[e], Jeffrey G. Reid[f], Erica Tworog-Dube[b], Margaret B. Morgan[f], Donna M. Muzny[f], Lincoln Stein[e], John D. McPherson[e], Amy E. Roberts[g], Richard A. Gibbs[f], Benjamin G. Neel[d,1,2], and Raju Kucherlapati[a,b,1,2]

[a]Department of Genetics, Harvard Medical School, Boston, MA 02115; [b]Department of Medicine, Division of Genetics, Brigham and Women's Hospital, Boston, MA 02115; [c]Institute of Clinical Medicine, National Cheng Kung University Hospital, College of Medicine, National Cheng Kung University, Tainan 70457, Taiwan; [d]Princess Margaret Cancer Center, University Health Network, and Department of Medical Biophysics, University of Toronto, Toronto, ON, Canada M5G 1L7; [e]Ontario Institute for Cancer Research, Toronto, ON, Canada M5G 0A3; [f]Human Genome Sequencing Center, Baylor College of Medicine, Houston, TX 77030; and [g]Department of Cardiology and Division of Genetics, Department of Medicine, Boston Children's Hospital Boston, Boston, MA 02115

Noonan syndrome (NS) is a relatively common genetic disorder, characterized by typical facies, short stature, developmental delay, and cardiac abnormalities. Known causative genes account for 70–80% of clinically diagnosed NS patients, but the genetic basis for the remaining 20–30% of cases is unknown. We performed next-generation sequencing on germ-line DNA from 27 NS patients lacking a mutation in the known NS genes. We identified gain-of-function alleles in Ras-like without CAAX 1 (*RIT1*) and mitogen-activated protein kinase kinase 1 (*MAP2K1*) and previously unseen loss-of-function variants in RAS p21 protein activator 2 (*RASA2*) that are likely to cause NS in these patients. Expression of the mutant *RASA2*, *MAP2K1*, or *RIT1* alleles in heterologous cells increased RAS-ERK pathway activation, supporting a causative role in NS pathogenesis. Two patients had more than one disease-associated variant. Moreover, the diagnosis of an individual initially thought to have NS was revised to neurofibromatosis type 1 based on an *NF1* nonsense mutation detected in this patient. Another patient harbored a missense mutation in *NF1* that resulted in decreased protein stability and impaired ability to suppress RAS-ERK activation; however, this patient continues to exhibit a NS-like phenotype. In addition, a nonsense mutation in *RPS6KA3* was found in one patient initially diagnosed with NS whose diagnosis was later revised to Coffin–Lowry syndrome. Finally, we identified other potential candidates for new NS genes, as well as potential carrier alleles for unrelated syndromes. Taken together, our data suggest that next-generation sequencing can provide a useful adjunct to RASopathy diagnosis and emphasize that the standard clinical categories for RASopathies might not be adequate to describe all patients.

human genetics | developmental diseases | whole exome sequencing | PTPN11 | RAS

G erm-line mutations in genes encoding RAS-ERK signaling pathway components cause a set of related, autosomal dominant developmental disorders, termed "RASopathies" (1–3), which include Noonan syndrome (NS), Noonan syndrome with multiple lentigines (NS-ML; formerly known as LEOPARD syndrome), cardio-facio-cutaneous syndrome (CFCS), Costello syndrome (CS), and neurofibromatosis type 1 (NF-1). RASopathy patients typically display short stature, facial dysmorphia, cardiac defects, developmental delay, and other variably penetrant features. Some (e.g., NS, CS) RASopathies are associated with increased cancer predisposition, but the associated malignancies are distinct. The shared syndromic features of the RASopathies probably reflect ERK hyperactivation, although for NS-ML, at least some phenotypes result from excessive AKT-mTOR activity (4, 5). Inter- and intrasyndromic differences are probably due to the distinct effects of specific mutations, modifier alleles, and/or complexities in feedback regulatory pathways in various cell types. Delineating the genetics and biochemistry of RASopathies should shed light on normal human development and disease.

NS, the most common RASopathy, occurs in familial and sporadic forms and is characterized by typical facies, short stature, variable developmental delay, cognitive defects, and cardiac abnormalities. Webbed neck, pectus abnormalities, coagulation defects, and cryptorchidism also are common (1). The heart defects, primarily pulmonary valve stenosis and hypertrophic cardiomyopathy (affecting ∼50% and 20–30% of individuals, respectively), usually are mutually exclusive and represent the primary cause of morbidity and mortality in NS patients (6). After the discovery of *PTPN11* mutations as the most common cause of NS (50%), *SOS1* (10–15%), *KRAS* (∼2%), *NRAS* (<1%), *SHOC2* (<1%), *CBL* (<1%), and *RAF1* (5–10%) were identified as additional genes for NS or NS-like disorders (7–16). Together, these genes account for ∼80% of clinically diagnosed NS patients.

Identifying the remaining NS genes is important for accurate diagnosis, patient management, and delineating genotype/phenotype relationships. We used next-generation sequencing (NGS) to analyze germ-line DNA in a cohort of NS patients who had been evaluated by a single clinician and lacked mutations in the known NS genes. Here we report the identification of additional candidate genes that, when mutated, are likely to cause NS.

Significance

Noonan syndrome (NS) is one of several RASopathies, which are developmental disorders caused by mutations in genes encoding RAS-ERK pathway components. The cause of 20–30% of NS cases remains unknown, and distinguishing NS from other RASopathies and related disorders can be difficult. We used next-generation sequencing (NGS) to identify causative or candidate genes for 13 of 27 NS patients lacking known NS-associated mutations. Other patients harbor single variants in potential RAS-ERK pathway genes, suggesting rare private variants or other genetic mechanisms of NS pathogenesis. We also found mutations in causative genes for other developmental syndromes, which together with clinical reevaluation, prompted revision of the diagnosis. NGS can aid in the challenging diagnosis of young patients with developmental syndromes.

MEDICAL SCIENCES

Results and Discussion

Previously Unidentified NS Genes. We identified a cohort of 27 NS patients without a known NS gene mutation. Whole exome sequencing (WES) was performed on DNA from 25 patients; the other two samples were analyzed by whole genome sequencing (WGS; see *SI Materials and Methods* for details). The average coverage of each base pair in the coding regions of WES was 55-fold, and the average coverage for WGS was 22-fold (Fig. S1). Single nucleotide variants (SNVs) were detected and filtered for novel, missense, and nonsense variants. On average, there were 121 novel nonsynonymous coding SNVs per individual analyzed by WES (Table S1).

Because all known NS mutations affect RAS-ERK pathway components, we hypothesized that the remaining NS genes were likely to affect this pathway. We compared variants identified by WES and WGS against a database containing genes known to be involved in the RAS-ERK pathway (Table S2) and/or that encode proteins belonging to a functional interaction network with RAS-ERK pathway components (*Materials and Methods* and Fig. S2). This filtering strategy helped us to identify genes with novel variants in multiple individuals with NS, including *RASA2*, *RIT1*, and *NF1*, as well as genes with variants in a single individual, including *MAP2K1*, *MAP3K8*, and *SPRY1* (Table S3).

Variants in Genes Associated with Other Syndromes. Distinguishing RASopathies from other developmental disorders with overlapping symptoms is a challenge, especially in young patients, because differentiating features can manifest later in life. While analyzing our cohort of patients diagnosed clinically with NS, we discovered variants associated with distinct syndromes, including other RASopathies and unrelated disorders.

NF1. Two patients (NS48 and NS166) had novel *NF1* mutations. Patient NS48 was first examined at the age of 18 mo. Although the initial clinical diagnosis was ambiguous, NS was considered a possibility based on pectus excavatum and consistent facial features. WES detected a nonsense mutation (p.1869*) in exon 38. After identifying this mutation, we learned that reexamination of the patient at the age of 22 mo revealed café au lait macules and axillary freckling characteristic of NF-1, and his diagnosis had been revised to neurofibromatosis-NS [NFNS; Mendelian Inheritance in Man (MIM) MIM 601321] (17).

Patient NS166 had a missense variant (p.L1361R) in exon 30 (Table S3, Fig. 1*A*, and Fig. S3*A*). *NF1* encodes neurofibromin, a RAS-GTPase-activating protein (RAS-GAP). Although most

causative *NF1* point mutations result in premature translation termination (18), some disease-associated missense mutations encode unstable NF1 proteins without affecting *NF1* mRNA levels (19), and others impair RAS-GAP activity (20–22). The leucine at position 1361 of NF1 is located in the GAP-related domain (NF1-GRD) and is highly conserved (Fig. 1*B* and Fig. S3 *B* and *C*). The nonconservative amino acid substitution (p.L1361R) in patient NS166 is considered highly likely to be damaging [multivariate analysis of protein polymorphism (MAPP) $P = 1.8 \times 10^{-5}$]. To assess the biochemical effects of this mutation, we compared the effects of a v-myc avian myelocytomatosis viral oncogene homolog (MYC) epitope-tagged, WT NF1-GRD construct (amino acids 1187–1574) to MYC-NF1-GRD bearing the p.L1361R mutation. Transient transfection of each construct into HEK293T cells resulted in similar levels of *NF1-GRD* mRNA (Fig. 1*C*), but compared with WT NF1-GRD, the level of the mutant NF1-GRD protein was markedly decreased (Fig. 1*D*). These results suggest that the p.L1361R mutation decreases protein stability, as seen with other *NF1* missense mutations (19). Accordingly, the mutant NF1-GRD construct was defective in suppressing basal and epidermal growth factor (EGF)-evoked ERK activation, as assessed by immunoblotting with anti–phosphorylated-ERK (p-ERK) antibodies (Fig. 1*D*).

Like NS48, NS166 only showed NS features at the time of enrollment into our study at the age of 23 (Table S3). She is now 27 y old and has a single café au lait macule, no inguinal or axillary freckling, no neurofibromas, no Lisch nodules, and no other classic features of NF-1. Such features would have been expected to appear by age 10, and thus NS166 does not meet the clinical diagnostic criteria for NF-1, despite her *NF1* mutation.

Previous studies identified patients with features of NS and NF1; subsequent sequence analyses indicated that such patients almost always have an *NF1* mutation (23). NS166 appears to fall into this category, although notably, this patient displayed no obvious NF-1–specific symptoms, as has also been reported recently for another individual (24). The presence of the *NF1* mutation suggests that she should be monitored for the potential long-term complications of NF-1 rather than NS. Also, because of the frequency with which we identified *NF1* mutations in this cohort, it might be advisable to add *NF1* to RASopathy gene panels in clinical diagnostic laboratories.
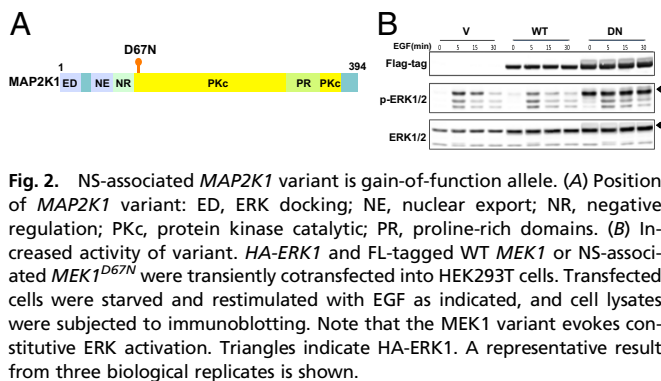
RPS6KA3. We detected a nonsense mutation in *RPS6KA3* in one individual (NS24; Table S3 and Fig. S4). Mutations in *RPS6KA3*, encoding RSK2, cause Coffin–Lowry syndrome (CLS), a very rare X-linked dominant genetic disorder (estimated incidence: 1 in 50,000–100,000) that features severe psychomotor retardation, facial and digital dysmorphism, progressive skeletal deformation, and cardiac defects (25). NS24 was diagnosed with NS when enrolled in our cohort at age 1 y due to typical facies, short stature, congenital heart defect, and developmental delay, but his facial features later evolved. CLS was suspected at age 9 y and was confirmed by *RPS6KA3* sequencing.

Probable Causative Variants Associated with NS Patients. *MEK1 gain-of-function mutation.* We detected a mutation (p.D67N) in *MAP2K1*, which encodes MEK1, in patient NS53 (Table S3, Fig. 2*A*, and Fig. S5). This mutation was reported previously in one CFCS case and two NS cases, but its biochemical activity had not been well characterized (26). Expression of MEK1^{D67N} caused constitutive ERK activation in transiently transfected human embryonic kidney 293T (HEK293T) cells; under the same conditions, WT MEK1 had little effect (Fig. 2*B*). These data identify *MAP2K1^{D67N}* as the causative allele in this patient.

RIT1 gain-of-function mutations. We identified five individuals (NS03, NS36, NS78, NS87, and NS92) who had missense mutations in *RIT1* (p.A57G, p.A77P, p.F82V, and p.G95A) and confirmed them by Sanger sequencing (Fig. 3*A* and Fig. S6*A*). RIT1 belongs to the RAS superfamily of small GTPases, and is >50% identical to RAS. Previous studies showed that an activated mutant of RIT1 (p.Q79L) can increase p38 MAPK and/or ERK activation in a cell-specific manner (27). The NS-associated mutations localize
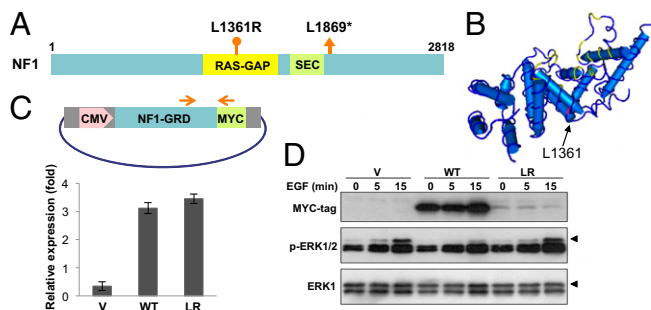
Fig. 1. NS-associated *NF1* variants are loss-of-function alleles. (*A*) Variants found in NS patients: RAS-GAP, RAS-GTPase activating protein-related; SEC, Sec14p-like lipid-binding domain. (*B*) NS-associated residue (pink) maps to RAS-GAP domain. RAS binding sites are in yellow. (*C*) WT and mutant *NF1-GRD* constructs express similar mRNA levels following transient transfection. Real-time qPCRs were performed using the indicated primers (arrows). (*D*) NS-associated *NF1* variant encodes unstable protein. HEK293T cells were cotransfected with expression constructs for *HA-ERK1* and WT *NF1-GRD* or *NF1-GRD^{L1361R}*, starved, and restimulated with EGF. Lysates were immunoblotted, as indicated. Note decreased level of the mutant and its inability to inhibit EGF-evoked ERK activation. Triangles show HA-ERK1. A representative result from three biological replicates is shown.

Fig. 2. NS-associated *MAP2K1* variant is gain-of-function allele. (*A*) Position of *MAP2K1* variant: ED, ERK docking; NE, nuclear export; NR, negative regulation; PKc, protein kinase catalytic; PR, proline-rich domains. (*B*) Increased activity of variant. HA-ERK1 and FL-tagged WT *MEK1* or NS-associated *MEK1^{D67N}* were transiently cotransfected into HEK293T cells. Transfected cells were starved and restimulated with EGF as indicated, and cell lysates were subjected to immunoblotting. Note that the MEK1 variant evokes constitutive ERK activation. Triangles indicate HA-ERK1. A representative result from three biological replicates is shown.

to the G2 domain (A57), G3 domain (A77), and switch II region (F82 and G95), which are conserved across vertebrates (Fig. 3*A* and Fig. S6*B*). Although the p.A57G mutant is not predicted to be damaging (MAPP *P* = 0.508), the other three alleles (p.A77P, p.F82V, and p.G95A) are expected to significantly affect protein function (MAPP *P* = 1.066×10^{-4}, 0.002, and 0.009, respectively).

To assess their effects on signaling, we recombined Flagged tagged (FL-) versions of each variant, as well as known activated (Q79L) and impaired (S35N) *RIT1* mutants (27), into Flp-In T-REx 293 cells. This cell system enables tetracycline-inducible expression of constructs integrated into the same locus. Exogenous FL-RIT1 expression was induced for 24 h, after which we assessed ERK and p38 activation in unsynchronized cells (NS), in starved cells (0), or in starved cells restimulated with EGF for various times, using immunoblotting with appropriate phospho-specific antibodies. All of the mutant-expressing cells showed enhanced p-ERK levels (compared with WT RIT1-expressing cells) under unsynchronized conditions (Fig. 3*B*). EGF-induced ERK activation also was enhanced and/or sustained in cells expressing three (A57G, A77P, and F82V) of the mutants (Fig. 3*B*). RIT1^{G95A}-expressing cells did not show consistent EGF-induced ERK hyperactivation (Fig. 3*B*), nor was p38 activity affected consistently by any of the RIT1 mutants (Fig. S6*C*). Notably, expression of RIT1^{S35N}, a presumptive dominant negative mutant analogous to RAS^{N17} (27), did not impair basal or EGF-induced ERK activation. These data suggest that RIT1 does not play a major role in normal RAS-ERK pathway activation, at least in Flp-In T-REx293 cells; i.e., the NS-associated mutants act as neomorphs. We also observed increased levels of most of the RIT1 mutants (except p.G95A) compared with WT RIT1 (Fig. 3*B*). However, cycloheximide experiments indicated that the half-lives of two (p.A77P and p.F82V) of the NS-associated RIT1 mutant proteins, as well as that of the known activated mutant p.Q79L, were prolonged, suggesting a potential mechanism for their increased ability to promote ERK activation (Fig. 3*C* and Fig. S7). By contrast, the half-life of p.A57G was only minimally prolonged, despite its increased steady-state levels. Taken together, our data support the conclusion that *RIT1* is a causative gene for NS.
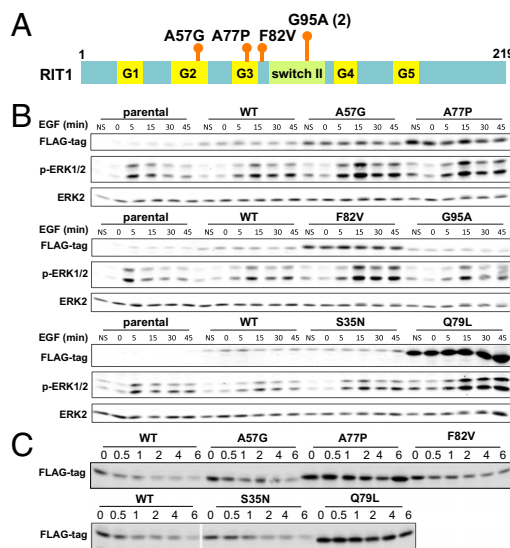
While this manuscript was in preparation, Aoki et al. reported *RIT1* mutations in NS (28). Our results clearly validate *RIT1* as a causative gene for NS. In their study, hypertrophic cardiomyopathy (HCM), which affects only ~20% of NS patients overall, was seen in 70% of cases with a *RIT1* mutation. We did not find such a correlation, perhaps because our cohort was relatively small. Alternatively, increased HCM incidence might correlate with *RIT1* mutations only in Asian NS patients; notably, strain background can strongly affect the penetrance of NS phenotypes in mouse models (29). Aoki et al. also did not see consistent hyperactivation of ERK in heterologous cells expressing NS-associated RIT1 mutants. This discrepancy with our results could reflect the use of different cell systems; specifically, we used stable cell lines that inducibly express mutant alleles at near-physiological levels, which could reveal subtle signs of RAS-ERK
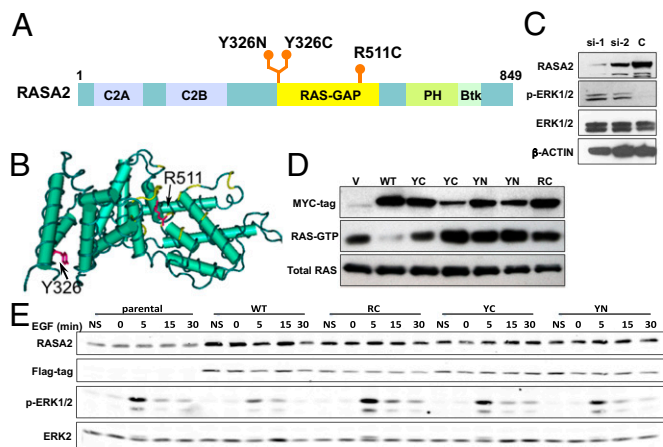
pathway activation that are missed in transient transfection studies. Moreover, we found that, compared with WT RIT1, some gain-of-function RIT1 proteins exhibit enhanced stability (Fig. 3*D*); hence, normalizing the effects of RIT1 variants to protein expression can underestimate their biological effects.

The germ-line *RIT1* alleles that we identified also have been reported as somatic mutations in cancer. The p.A77P variant has been detected in lung adenocarcinoma (COSMIC), and p.F82V was recently identified in leukemia (30, 31). The latter finding is of substantial interest, given the association between NS and juvenile myelomonocytic leukemia (JMML) (1). Although the two patients carrying RIT1 p.A77P and p.F82V in our study have no evidence of cancer, given the above associations, it will be important to follow them closely for potential malignancies.

***RASA2* loss-of-function variants.** Three patients (NS06, NS16, and NS78) had novel missense variants, affecting two residues in RASA2 (Fig. 4*A* and Fig. S8*A*), the mammalian RAS-GAP family member with highest similarity to *Drosophila* Gap1 (32). The NS-associated alterations (p.Y326C, p.326N, and p.R511C) alter highly conserved amino acids in the GAP domain of RASA2, which itself is highly conserved (Fig. S8 *B* and *C*). Modeling the RASA2 mutants on the structure of p120GAP predicts that R511 is a direct contact site for RAS (Fig. 4*B*) (33), and the NS-associated mutations are expected to damage RASA2 function (MAPP *P* = 2.12×10^{-5}, 9.42×10^{-5}, and 5.39×10^{-6}, respectively).

We tested the role of RASA2 in RAS-ERK pathway regulation by knockdown experiments. Decreasing RASA2 levels in

Fig. 3. NS-associated *RIT1* mutants activate RAS-ERK pathway. (*A*) Positions of variants are shown. Like all RAS family members, RIT1 contains five conserved functional domains: phosphate binding (G1 and G3), GTP binding and hydrolysis (G4 and G5), and effector protein binding (G2). Switch II indicates region homologous to switch II domain in RAS. (*B*) Representative immunoblots of lysates from cell lines expressing FL-tagged WT RIT1 or RIT variants, which were either nonsynchronized (NS) or starved (0) and then restimulated with EGF as indicated, lysed, and immunoblotted. Note increased basal and/or stimulated ERK1/2 phosphorylation in RIT1 mutant (AG, AP, FV, and GA) compared with WT RIT1-expressing cells. Lysates from cells expressing dominant-negative RIT1 (SN) or known activating mutant (QL) are also shown. Representative result from three independent biological replicates. (*C*) Representative immunoblots of lysates from cell lines expressing FL-tagged WT RIT1 or RIT variants, treated with cycloheximide, and then harvested, as indicated. Lysates from 1.5×10^5 (AG, AP, FV, and QL) or 3×10^5 (WT and SN) cell equivalents were immunoblotted with anti-FLAG antibodies. Note the increased stability of RIT1 mutants compared with WT or SN RIT. Also see Fig. S7.

Fig. 4. NS-associated *RASA2* variants are loss-of-function alleles. (*A*) Positions of variants: C2A, C2 domain first repeat; C2B, C2 domain second repeat; RAS-GAP, RAS-GTPase activating protein; PH, Pleckstrin homology-like; BTK, Bruton's tyrosine kinase cysteine-rich motif. (*B*) NS-associated residues (pink) map to RAS-GAP domain. Note that R511 is a putative RAS binding site (yellow). (*C*) *RASA2* depletion enhances ERK1/2 activation. HEK293T cells transfected with either of two siRNAs for 48 h were lysed and immunoblotted. Note that increased ERK1/2 phosphorylation in *RASA2*-depleted cells correlates inversely with RASA2 level, with ∼50% reduction in RASA2 increasing ERK activation. (*D*) NS-associated RASA2 variants have defective GAP activity. Activated RAS levels in HEK293T cells transiently transfected with *MYC*-tagged WT *RASA2* or NS-associated *RASA2* variant (YC, YN, and RC) constructs were measured by RAF-RBD binding. Note that WT RASA2 suppresses, whereas NS-associated RASA2 variants enhance, RAS activation compared with controls. (*E*) Cell lines expressing Flag-tagged WT RASA2 or the indicated RASA2 variants (YC, YN, and RC) were starved and then restimulated with EGF. Lysates were immunoblotted, as indicated. A representative result from three biological replicates is shown.

HEK293T cells with either of two siRNAs increased p-ERK levels, and the extent of ERK activation was inversely related to the residual level of RASA2 (Fig. 4*C*). Notably, lowering RASA2 levels by only ∼50% (si-2), as would be expected in a NS patient with a heterozygous inactivating *RASA2* mutation, significantly increased p-ERK levels in EGF-stimulated cells (Fig. 4*C*). Next, we tested the impact of the NS-related RASA2 variants on GAP activity. HEK293T cells transiently transfected with a *MYC-RASA2* expression construct showed barely detectable RAS-GTP, as monitored by RAF-RBD binding (Fig. 4*D*). By contrast, expression of the RASA2 variants not only failed to decrease RAS activity, but increased RAF-RBD binding compared with control vector (V)-transfected cells (Fig. 4*D*). In Flp-In T-REx 293 cells, WT RASA2 suppressed EGF-induced ERK activation compared with parental cells. By contrast, neither RASA2^{Y326C} nor RASA2^{Y326N} suppressed ERK activation (Fig. 4*E*), whereas RASA2^{R551C} expression actually enhanced p-ERK levels, suggesting that this variant has dominant negative effects (Fig. 4*E*).

Parental DNA was not available for the patients bearing RASA2 variants. Moreover, given that NS is an autosomal dominant disease with incomplete penetrance, parental DNA results might not be dispositive. Nevertheless, our functional data nominate *RASA2* as a new causative gene for NS. All of our patients are heterozygous for their *RASA2* allele, suggesting haploinsufficiency, a previously unreported mechanism of NS pathogenesis. However, one RASA2 variant, p.R511C, appears to have dominant negative effects. The physiological role of RASA2 remains largely unknown, although our results implicate it in EGF-induced RAS-ERK activation in some cell types. Accordingly, EGF induces rapid, PI3 kinase-dependent recruitment of RASA2 from the cytosol to the plasma membrane in rat pheochromocytoma cells (34). Notably, 54 missense and nonsense mutations [compared with 17 synonymous mutations, as listed on the Catalogue Of Somatic Mutations In

Cancer (COSMIC) database (http://cancer.sanger.ac.uk/cancergenome/projects/cosmic/)] in *RASA2* have been identified in various malignancies, including cervical, colorectal, lung, and endometrial cancer (overall incidence, 0.65%). These data suggest that *RASA2* might be a tumor suppressor gene and suggest that NS patients carrying *RASA2* mutations also should be monitored for cancer.

Other Potential NS Candidate Genes. *SPRY1 loss-of-function mutation.* We identified a nonsense allele (pE79*) of *SPRY1* in NS17 (Table S3 and Fig. S4). SPRY1 is a negative regulator of the RAS-ERK pathway, which reportedly binds to SHP2 (encoded by *PTPN11*) and RAF1 through its cysteine-rich domain (CRD) and inhibits ERK activation via an as yet unclear mechanism (35). The nonsense variant encodes a truncated version of SPRY1 that retains its Casitas B-lineage lymphoma (CBL) tyrosine kinase-binding (TKB) motif but lacks the serine-rich domain and CRD; hence, the predicted SPRY1 truncation in NS17 might be functionally defective. *Spry1*$^{-/-}$ mice have kidney defects and decreased viability, but no features characteristic of NS were reported. *Spry1*$^{+/-}$ mice reportedly are normal (36), although NS phenotypes in the mouse could be subtle and difficult to detect. Notably, NS17 has a healthy heart, normal height, and only very mild facial dysmorphia and learning problems, which might be caused by the SPRY1 pE79* variant. Nevertheless, further studies are needed to clarify the potential pathogenic role of the truncated SPRY1.

MAP3K8. We detected one missense *MAP3K8* variant, encoding p.L128V, in NS49 (Table S3 and Fig. S4). *MAP3K8* (a.k.a. *TPL2, COT*) is an oncogene encoding a MAP kinase kinase kinase (MEKK) that can phosphorylate and activate MEK (37). An activating MAP3K8 allele might be expected to cause NS-like phenotypes. However, the NS49 variant is conservative and occurs in a region of unknown function. When we expressed WT or mutant MAP3K8 in Flp-In T-REx 293 cells, each constitutively activated ERK (Fig. S9). Although *MAP3K8* remains an attractive candidate NS gene for this patient, further analysis will be required to establish its pathogenic significance.

We also identified more than one variant in other genes with a potential relationship to the RAS-ERK pathway in 14 NS individuals (Table S4). The pathologic significance of these variants awaits further, more detailed, biochemical and biological analysis.

Compound Mutations in NS Individuals. We found that all 27 patients have variants in more than one gene classified as being involved in the RAS-ERK pathway. In most cases, we think it likely that their symptoms are caused by only one of these variants. However, in two cases, we suspect that both alleles contribute to their clinical features.

Patient NS78 had RIT1 p.F82V and RASA2 p.Y326C alleles (Table S3). As discussed above, both of these variants cause increased ERK activation in transfected heterologous cells. Co-occurring mutations in NS-causing genes have been reported in a few patients with NS (38–40). Additive or modifying effects were observed in a NS patient carrying *SHOC2* and *PTPN11* mutations and in another individual harboring *PTPN11* and *KRAS* mutations. By contrast, no atypical phenotypes were observed in a patient with *PTPN11* and *SOS1* mutations. NS78 has the typical facial dysmorphia seen in NS, as well as short stature, developmental delay, atrial septal defect, and pulmonary valve stenosis. Patients carrying single variant alleles in *RASA2* or *RIT1* showed typical facial, developmental and cardiac phenotypes (Fig. S10 and Table S3). NS78 also shows defects that occur infrequently in NS, such as branch pulmonary artery stenosis and a dilated main pulmonary artery (Table S3). It is possible that the atypical cardiac phenotypes in NS78 result from the combined effects of the *RIT1* and *RASA2* variants. However, because of the small size of our cohort, we could not assign genotype-phenotype associations in patients with *RIT1* or *RASA2* variants. Analysis of a larger cohort will be necessary to clarify the distinct roles of RIT1 or RASA2 in NS pathogenesis.

Patient NS87 had RIT1 p.G95A and a novel TGFB2 p.A251S allele (Table S3). *TGFB2* mutations cause Marfan syndrome-associated familial thoracic aortic aneurysms and dissections (TAADs) (41, 42). Interestingly, NS87 had cardiac abnormalities, including atrial fibrillation and pulmonary artery aneurysms, which are not typical of NS (Table S3). Whether the variants in *TGFB2* or *RIT1*—or both—contribute to these defects is unclear. On detection of the variant *TGFB2* allele, we attempted to contact the participant only to learn she had passed away in her early 50s (no details known).

Other Variants of Potential Pathogenic Significance. While searching for genes classified as involved in the RAS-ERK pathway, we incidentally identified multiple variants in genes linked to other syndromes. Two patients (NS100 and NS110) harbored novel variants in *FRAS1* (Table S3 and Fig. S4), a causative gene for Fraser syndrome (MIM 219000), an autosomal recessive disorder characterized by cryptophthalmos and other malformations (43). Fraser syndrome is quite rare (incidence ~1 in 250,000 live births and 1 in 10,000 still births), and therefore the carrier frequency is expected to be 1/100~1/500. Although the mutations identified in this study (p.A713T and p.R1891H) are not predicted to be damaging (MAPP $P = 0.65$ and 0.9, respectively), one is located in the conserved furin protease (FU) domain and the other in a domain homologous to the chondroitin sulfate proteoglycan (CSPG) motifs of the NG2 protein (Fig. S4). The latter domain is the most frequently mutated region of *FRAS1* in Fraser syndrome (43). Although NS100 and NS110 are potential carriers for a disease-causing *FRAS1* allele, the role, if any, of these mutations in the NS phenotype of these patients is unclear.

We also identified novel missense variants in *VWF* (encoding p.V546G and p.R760L) in two patients (NS03 and NS123; Table S3 and Fig. S4). von Willebrand factor (*VWF*) encodes a large multimeric glycoprotein important for normal hemostasis (44). Heterozygous VWF mutations can cause von Willebrand disease (VWD; MIM 613160), a common hereditary bleeding disorder. Both variants in our NS patients map to the propeptide region of VWF that is involved in multimerization before its cleavage to produce mature VWF (44). The p.R760L, but not the p.V546G, variant is predicted to be damaging (MAPP $P = 1.74 \times 10^{-4}$ and 0.1294, respectively). Moreover, a missense mutation at arginine 706 (p.R760H), associated with quantitative deficiency of VWF, has been reported in a patient with VWD (45). Patient NS03, who carries VWF p.V546G, reported easy bruising but no overt bleeding problems. NS123, who carries VWF p.R760L, has not reported bleeding symptoms.

Finally, we observed multiple heterozygous variants in genes linked to other genetic syndromes in our cohort of NS patients (Table S5). With the exception of a single *MYO7A* allele found in autosomal recessive Usher syndrome (MIM 276903), the pathogenic significance of these alleles remains unknown.

Summary and Perspective. Managing patients with genetic defects requires accurate diagnosis. By performing NGS on 27 NS patients lacking known NS-associated mutations, we identified causative or candidate genes in 13 of 27 NS cases (48%). All of the 13 NS cases are nonfamilial based on clinical diagnosis. However, we could not be certain if these mutations occurred de novo or were inherited because parental DNA samples were not available. As NS is a heterogeneous disorder with variable phenotypic expression, inherited cases might remain unidentified because the affected parent exhibits subtle syndromic phenotypes. The remaining patients harbor single variants in genes encoding potential RAS-ERK pathway members, but the lack of recurrent alleles in these genes suggests that the remaining causes of NS could be rare, potentially private, variants or other genetic mechanisms (e.g., copy number alteration, regulatory region mutations). In this regard, this developmental syndrome resembles many cancers, with a few common driver mutations and a long "tail" of more rare causative variants. Unexpectedly, we also identified mutations in genes associated with other developmental syndromes, which together with clinical reevaluation, prompted a change in diagnosis. Our results indicate that NGS can aid in the often challenging differential diagnosis of young patients with developmental syndromes.

Because the RAS-ERK pathway is best known for its involvement in cancer, drugs that inhibit pathway components are in use or under development (46). Such drugs also could be useful for treating RASopathy patients. Identifying the causative allele in each NS patient is likely to be critical for choosing an effective therapy. For example, mice that carry a *Sos1* mutation develop multiple NS features, and these defects can be prevented or their expression reduced by MEK inhibitor treatment during the early stages of life (47). Postnatal MEK inhibitor treatment also reverses some NS symptoms in *Raf1* mutant mice (48), and rapamycin normalizes HCM in LS mouse models (5). Analogous models for the new NS genes defined here and by others (28) could prove important for personalizing RASopathy therapy.

Materials and Methods

Patient Samples. This study was approved by the Institutional Review Boards of Partners HealthCare, Boston, and Boston Children's Hospital with informed consent and assent (when applicable). Enrollees were given a clinical diagnosis of NS by a medical geneticist. Each was examined and had records reviewed by A.E.R. (75%) or had photos and records evaluated by A.E.R. (25%). Inclusion criteria were based on the van der Burght system (49). Genomic DNA was extracted from whole blood or another tissue from each enrollee. Participants had the option of whether or not to receive research results of NS causative genes. Most enrollees consented before the advent of exome and genome sequencing. To help guide reporting of unanticipated, medically actionable results (e.g., *VWF* variants) and recessive disease carrier status (e.g., *FRAS* variants), we consulted our Institutional Review Board and used the American College of Medical Genetics (ACMG) Recommendations for Reporting of Incidental Findings in Clinical Exome and Genome Sequencing (50).

Exome Sequencing and Mutation Identification. Genomic DNA libraries were prepared and captured as described in *SI Materials and Methods*. Samples were sequenced on an ABI SOLiD (23 cases) or an Illumina Genome Analyzer II (4 cases). Sequencing reads were aligned to human genome Hg18 with Novoalign. Samtools, picard, and the Genome Analysis Toolkit (GATK) (51) were used to search for SNVs, allowing three mismatches in 50 nucleotides. To enable additional filtering with the newest dbSNP137, the output was lifted to human genome Hg19 using GATK liftOverVCF, and variants were annotated with SeattleSeqAnnotation 137. The potential impact of amino acid changes (MAPP P value) was assessed with ProPhylER (52). Variants were viewed manually on integrative genomics viewer (igv) to eliminate strand bias and reduce false positive calls.

Identification of Candidate Genes for NS. We surveyed 789 genes (listed in Table S2) thought to be involved in RAS-ERK pathway regulation from the literature and the GeneAssist pathway Altas. A protein functional interaction (FI) network was also used to analyze sequencing data (53). Seven known NS-associated genes (*PTPN11, KRAS, NRAS, RAF1, BRAF, SOS1,* and *SHOC2*) served as seeds to find intermediate-related genes, such that the seeds were connected by intermediate genes either known to be direct interactors or interactors that require one linker (Fig. S2A). Intermediate genes were extracted from the FI network. Genes that were one-hop-away from the seven NS genes were assigned a higher priority for testing (Fig. S2*B*).

Cloning NS Variants. NF1-GAP was cloned by RT-PCR from human cardiac cDNA (Invitrogen). *MAP2K1, RIT1,* and *RASA2* cDNAs (from Open Biosystems, Clontech, or Transomics, respectively) were amplified by PCR, with the addition of a Flag tag at their N termini or a MYC tag at their C termini (StrataClone;l Agilent). Amplified fragments were subcloned into pcDNA5/FRT/TO (Invitrogen) to generate Flp-In T-REx 293 cell lines. NS-associated mutants were generated by site-directed mutagenesis. Primers and PCR conditions are available from P.-C.C. and J.Y. on request.

Cell Lines, Transfections, and Protein Analysis. Flp-In T-REx 293 cells (Invitrogen) were maintained in DMEM plus 10% (vol/vol) FBS and antibiotics. Lines expressing NS variants were generated by cotransfecting host cells with the Flp

recombinase-expressing plasmid pOG44 (Invitrogen) and the appropriate pcDNA5/FRT/TO expression plasmids, using FuGENE HD (Promega), as per the manufacturer. Transfected cells were selected in hygromycin (250 µg/mL). Expression of the indicated gene was induced by incubation with 1 µg/mL tetracycline for 24 h before analysis. For transient transfections, HEK293T cells (ATCC) were seeded in antibiotic-free media for 1 d and then transferred into Opti-MEM (Invitrogen). *RASA2* siRNAs (Ambion), WT, or NS mutant expression constructs were transfected into HEK293T cells, along with a hemagglutinin (HA)-ERK expression construct, using Lipofectamine 2000 (Invitrogen). Cells were starved in serum-free DMEM overnight, before stimulation with EGF (5–50 ng/mL, as indicated). Cell lysis, immunoprecipitations, immunoblotting, and quantification are detailed in *SI Materials and Methods*. To estimate the protein half-lives, Flp-In TREx 293 cells expressing WT or mutant Flag-RIT were induced with tetracycline

as above and then treated with 100 µg/mL cycloheximide. At intervals, cell lysates were prepared and analyzed by immunoblotting with anti-Flag antibodies.

1. Gelb BD, Tartaglia M (2006) Noonan syndrome and related disorders: Dysregulated RAS-mitogen activated protein kinase signal transduction. *Hum Mol Genet* 15(Spec No 2):R220–R226.
2. Aoki Y, Matsubara Y (2013) Ras/MAPK syndromes and childhood hemato-oncological diseases. *Int J Hematol* 97(1):30–36.
3. Rauen KA (2013) The RASopathies. *Annu Rev Genomics Hum Genet* 14:355–369.
4. Kontaridis MI, Swanson KD, David FS, Barford D, Neel BG (2006) PTPN11 (Shp2) mutations in LEOPARD syndrome have dominant negative, not activating, effects. *J Biol Chem* 281(10):6785–6792.
5. Marin TM, et al. (2011) Rapamycin reverses hypertrophic cardiomyopathy in a mouse model of LEOPARD syndrome-associated PTPN11 mutation. *J Clin Invest* 121(3):1026–1043.
6. Roberts AE, Allanson JE, Tartaglia M, Gelb BD (2013) Noonan syndrome. *Lancet* 381(9863):333–342.
7. Tartaglia M, et al. (2001) Mutations in PTPN11, encoding the protein tyrosine phosphatase SHP-2, cause Noonan syndrome. *Nat Genet* 29(4):465–468.
8. Roberts AE, et al. (2007) Germline gain-of-function mutations in SOS1 cause Noonan syndrome. *Nat Genet* 39(1):70–74.
9. Tartaglia M, et al. (2007) Gain-of-function SOS1 mutations cause a distinctive form of Noonan syndrome. *Nat Genet* 39(1):75–79.
10. Razzaque MA, et al. (2007) Germline gain-of-function mutations in RAF1 cause Noonan syndrome. *Nat Genet* 39(8):1013–1017.
11. Schubert S, et al. (2006) Germline KRAS mutations cause Noonan syndrome. *Nat Genet* 38(3):331–336.
12. Martinelli S, et al. (2010) Heterozygous germline mutations in the CBL tumor-suppressor gene cause a Noonan syndrome-like phenotype. *Am J Hum Genet* 87(2):250–257.
13. Cordeddu V, et al. (2009) Mutation of SHOC2 promotes aberrant protein N-myristoylation and causes Noonan-like syndrome with loose anagen hair. *Nat Genet* 41(9):1022–1026.
14. Cirstea IC, et al. (2010) A restricted spectrum of NRAS mutations causes Noonan syndrome. *Nat Genet* 42(1):27–29.
15. Niemeyer CM, et al. (2010) Germline CBL mutations cause developmental abnormalities and predispose to juvenile myelomonocytic leukemia. *Nat Genet* 42(9):794–800.
16. Pandit B, et al. (2007) Gain-of-function RAF1 mutations cause Noonan and LEOPARD syndromes with hypertrophic cardiomyopathy. *Nat Genet* 39(8):1007–1012.
17. Colley A, Donnai D, Evans DG (1996) Neurofibromatosis/Noonan phenotype: A variable feature of type 1 neurofibromatosis. *Clin Genet* 49(2):59–64.
18. Wallace MR, et al. (1990) Type 1 neurofibromatosis gene: Identification of a large transcript disrupted in three NF1 patients. *Science* 249(4965):181–186.
19. Kaufmann D, et al. (2001) Spinal neurofibromatosis without café-au-lait macules in two families with null mutations of the NF1 gene. *Am J Hum Genet* 69(6):1395–1400.
20. Klose A, et al. (1998) Selective disactivation of neurofibromin GAP activity in neurofibromatosis type 1. *Hum Mol Genet* 7(8):1261–1268.
21. Upadhyaya M, et al. (1997) Mutational and functional analysis of the neurofibromatosis type 1 (NF1) gene. *Hum Genet* 99(1):88–92.
22. Thomas L, et al. (2012) Assessment of the potential pathogenicity of missense mutations identified in the GTPase-activating protein (GAP)-related domain of the neurofibromatosis type-1 (NF1) gene. *Hum Mutat* 33(12):1687–1696.
23. De Luca A, et al. (2005) NF1 gene mutations represent the major molecular event underlying neurofibromatosis-Noonan syndrome. *Am J Hum Genet* 77(6):1092–1101.
24. Croonen EA, Yntema HG, van Minkelen R, van den Ouweland AM, van der Burgt I (2012) Patient with a neurofibromatosis type 1 mutation but a clinical diagnosis of Noonan syndrome. *Clin Dysmorphol* 21(4):212–214.
25. Trivier E, et al. (1996) Mutations in the kinase Rsk-2 associated with Coffin-Lowry syndrome. *Nature* 384(6609):567–570.
26. Nava C, et al. (2007) Cardio-facio-cutaneous and Noonan syndromes due to mutations in the RAS/MAPK signalling pathway: Genotype-phenotype relationships and overlap with Costello syndrome. *J Med Genet* 44(12):763–771.
27. Shi GX, Andres DA (2005) Rit contributes to nerve growth factor-induced neuronal differentiation via activation of B-Raf-extracellular signal-regulated kinase and p38 mitogen-activated protein kinase cascades. *Mol Cell Biol* 25(2):830–846.
28. Aoki Y, et al. (2013) Gain-of-function mutations in RIT1 cause Noonan syndrome, a RAS/MAPK pathway syndrome. *Am J Hum Genet* 93(1):173–180.
29. Araki T, et al. (2009) Noonan syndrome cardiac defects are caused by PTPN11 acting in endocardium to enhance endocardial-mesenchymal transformation. *Proc Natl Acad Sci USA* 106(12):4736–4741.
30. Gómez-Seguí I, et al. (2013) Novel recurrent mutations in the RAS-like GTP-binding gene RIT1 in myeloid malignancies. *Leukemia* 27(9):1943–1946.
31. Forbes SA, et al. (2011) COSMIC: Mining complete cancer genomes in the Catalogue of Somatic Mutations in Cancer. *Nucleic Acids Res* 39(Database issue):D945–D950.
32. Maekawa M, et al. (1994) A novel mammalian Ras GTPase-activating protein which has phospholipid-binding and Btk homology regions. *Mol Cell Biol* 14(10):6879–6885.
33. Scheffzek K, Lautwein A, Kabsch W, Ahmadian MR, Wittinghofer A (1996) Crystal structure of the GTPase-activating domain of human p120GAP and implications for the interaction with Ras. *Nature* 384(6609):591–596.
34. Lockyer PJ, et al. (1997) Distinct subcellular localisations of the putative inositol 1,3,4,5-tetrakisphosphate receptors GAP1IP4BP and GAP1m result from the GAP1IP4BP PH domain directing plasma membrane targeting. *Curr Biol* 7(12):1007–1010.
35. Guy GR, Jackson RA, Yusoff P, Chow SY (2009) Sprouty proteins: Modified modulators, matchmakers or missing links? *J Endocrinol* 203(2):191–202.
36. Basson MA, et al. (2005) Sprouty1 is a critical regulator of GDNF/RET-mediated kidney induction. *Dev Cell* 8(2):229–239.
37. Patriotis C, Makris A, Chernoff J, Tsichlis PN (1994) Tpl-2 acts in concert with Ras and Raf-1 to activate mitogen-activated protein kinase. *Proc Natl Acad Sci USA* 91(21):9755–9759.
38. Ekvall S, Hagenäs L, Allanson J, Annerén G, Bondeson ML (2011) Co-occurring SHOC2 and PTPN11 mutations in a patient with severe/complex Noonan syndrome-like phenotype. *Am J Med Genet A* 155A(6):1217–1224.
39. Brasil AS, et al. (2010) PTPN11 and KRAS gene analysis in patients with Noonan and Noonan-like syndromes. *Genetic Testing Molec Biomarkers* 14(3):425–432.
40. Brasil AS, et al. (2010) Co-occurring PTPN11 and SOS1 gene mutations in Noonan syndrome: Does this predict a more severe phenotype? *Arq Bras Endocrinol Metabol* 54(8):717–722.
41. Boileau C, et al.; National Heart, Lung, and Blood Institute (NHLBI) Go Exome Sequencing Project (2012) TGFB2 mutations cause familial thoracic aortic aneurysms and dissections associated with mild systemic features of Marfan syndrome. *Nat Genet* 44(8):916–921.
42. Lindsay ME, et al. (2012) Loss-of-function mutations in TGFB2 cause a syndromic presentation of thoracic aortic aneurysm. *Nat Genet* 44(8):922–927.
43. van Haelst MM, et al.; Fraser Syndrome Collaboration Group (2008) Molecular study of 33 families with Fraser syndrome new data and mutation review. *Am J Med Genet A* 146A(17):2252–2257.
44. Castaman G (2013) New development in von Willebrand disease. *Curr Opin Hematol* 20(5):424–429.
45. Riddell AF, et al. (2009) Characterization of W1745C and S1783A: 2 novel mutations causing defective collagen binding in the A3 domain of von Willebrand factor. *Blood* 114(16):3489–3496.
46. Schubert S, Shannon K, Bollag G (2007) Hyperactive Ras in developmental disorders and cancer. *Nat Rev Cancer* 7(4):295–308.
47. Chen PC, et al. (2010) Activation of multiple signaling pathways causes developmental defects in mice with a Noonan syndrome–associated Sos1 mutation. *J Clin Invest* 120(12):4353–4365.
48. Wu X, et al. (2011) MEK-ERK pathway modulation ameliorates disease phenotypes in a mouse model of Noonan syndrome associated with the Raf1(L613V) mutation. *J Clin Invest* 121(3):1009–1025.
49. van der Burgt I, et al. (1994) Clinical and molecular studies in a large Dutch family with Noonan syndrome. *Am J Med Genet* 53(2):187–191.
50. Green RC, et al. (2013) ACMG recommendations for reporting of incidental findings in clinical exome and genome sequencing. *Gen Med* 15(7):565–574.
51. McKenna A, et al. (2010) The Genome Analysis Toolkit: A MapReduce framework for analyzing next-generation DNA sequencing data. *Genome Res* 20(9):1297–1303.
52. Binkley J, et al. (2010) ProPhylER: A curated online resource for protein function and structure based on evolutionary constraint analyses. *Genome Res* 20(1):142–154.
53. Wu G, Feng X, Stein L (2010) A human functional protein interaction network and its application to cancer data analysis. *Genome Biol* 11(5):R53.